Received: 3 June 2022 | Revised: 15 July 2022 | Accepted: 19 July 2022

DOI: 10.1002/ardp.202200294

FULL PAPER

ARCH PHARM DPhG
Archiv der Pharmazie

Synthesis, anticholinesterase activity, molecular docking, and molecular dynamic simulation studies of 1,3,4-oxadiazole derivatives

Şeyma Durmaz[1] | Asaf E. Evren[2,3] | Begüm N. Sağlık[2] | Leyla Yurttaş[2] | Naime F. Tay[1]

[1]Department of Chemistry, Faculty of Science and Letters, Eskisehir Osmangazi University, Eskisehir, Turkey

[2]Department of Pharmaceutical Chemistry, Faculty of Pharmacy, Anadolu University, Eskişehir, Turkey

[3]Vocational School of Health Services, Department of Pharmacy Services, Bilecik Seyh Edebali University, Bilecik, Turkey

Correspondence
Naime F. Tay, Department of Chemistry, Faculty of Science and Letters, Eskisehir Osmangazi University, TR 26480 Eskisehir, Turkey.
Email: ftay@ogu.edu.tr

Funding information
Eskisehir Osmangazi Üniversitesi, Grant/Award Number: Project Number: 202019A106

Abstract

Two new series of 1,3,4-oxadiazoles bearing pyridine and thiazole heterocycles (**4a-h** and **5a-h**) were synthesized (2,5-disubstituted-1,3,4-oxadiazoles). The structures of these newly synthesized compounds were confirmed by ^{1}H nuclear magnetic resonance (NMR), ^{13}C NMR, high-resolution mass spectrometric and Fourier transform infrared spectroscopic methods. All these compounds were evaluated for their enzyme inhibitory activities against two cholinesterase enzymes, acetylcholinesterase (AChE) and butyrylcholinesterase (BChE). From the studies, we identified compounds **4a**, **4h**, **5a**, **5d**, and **5e** as selective AChE inhibitors, with IC_{50} values ranging from 0.023 to 0.037 µM. Furthermore, docking studies of these compounds were performed at the active sites of their target enzymes. The molecular docking study showed that **5e** possessed an ideal docking pose with interactions inside AChE.

KEYWORDS
anticholinesterase activity, molecular docking, molecular dynamics simulation, oxadiazole, pyridine

1 | INTRODUCTION

Acetylcholinesterase (AChE) is a member of the cholinesterase enzyme family, regulating acetylcholine, a neurotransmitter, through hydrolysis at neuromuscular junctions, thus proving itself to be an essential component in the maintenance and performance of nervous systems.[1–6] The other member of the cholinesterase enzyme family is butyrylcholinesterase (BChE).[1,7,8] AChE and BChE are responsible for the rapid hydrolysis of acetylcholine at synaptic clefts to produce choline and acetate products.[9] The point where the two enzymes differ from each other is that AChE is found primarily in the blood and neural synapses whereas BChE is found primarily in the liver and other organs, such as the intestine and heart.[7,9–12] Loss of cholinergic neurons resulting in reduced levels of the neurotransmitter acetylcholine in the brain is believed to be one of the causes of Alzheimer's disease (AD).[13] Results of experimental studies have shown that increases in AChE inhibition are associated with an overall improvement in cognitive function and capacity to perform activities of daily living in patients with AD.[12–18] One of the successful pharmacological approaches developed for symptomatic AD treatment today is focused on acetylcholinesterase inhibitors (AChEI). Three AChEI drugs are currently prescribed for AD treatment: donepezil, rivastigmine, and galantamine. In addition to AD, various ChE inhibitors have also proven to be effective for the treatment of glaucoma, myasthenia gravies, Parkinson's disease, and Down syndrome.[6,16,19]

In regard to the rationale for their use as a therapeutic intervention, AChEI contribute to improving cholinergic function by increasing the concentration of acetylcholine in the brain. When the interaction between AChE and donepezil was examined in X-ray, it

was determined that AChE has a narrow cavity that is divided into two parts: the esteratic (catalytic) site (CAS) and the peripheral anionic site (PAS). Molecular interactions with tryptophan, serine, and arginine amino acids via cation–π, covalent, and hydrogen bonding interactions are all essential for AChE inhibition activity. In the design of new AChEIs, studies on long-chain, unbranched molecular structures have been carried out, based on this approach.[20,21]

Compounds containing nitrogen heterocyclic ring systems are of great importance and have an essential role as therapeutic agents in biological systems and are commonly used in many commercial drugs. Among them, 1,3,4-oxadiazole derivatives are broadly investigated in pharmaceutical chemistry due to their various biological activities, such as anticancer,[21,22] anti-inflammatory,[23–25] analgesic agents,[26] and antimicrobial [27,28] activities. A related class of compounds of the 1,3,4-oxadiazoles is the oxadiazole-thiones (or thiols), which play an important role as intermediates in organic synthesis, theoretical chemistry, and biochemical studies. 1,3,4-Oxadiazole-2-thione derivatives have attracted the attention of researchers in recent years due to their wide pharmacological activities, such as anticancer,[29,30] antimicrobial,[31] antioxidant,[32] and AChEIs.[33,34]

Moreover, several derivatives of oxadiazole heterocycle bearing pyridine and thiazole rings with high inhibitory activity against metabolic enzymes, including human carbonic anhydrase I (hCA I), human carbonic anhydrase II (hCA II), AChE, BChE, and α-glucosidase have been reported.[35,36] Similarly, pyridine derivatives are other important biologically active heterocyclic compounds. Various pyridine derivatives are well known for their antioxidant, anti-inflammatory, antitubercular, and several other properties.[37–39] Furthermore, different moieties reported the development of new pyridine hybrids for the cholinesterase inhibitory activity.[40–46] Various pyridine-based drugs have been or are used in the treatment of AD, such as tacrine (AChEI) and umibecestat (BACE-1 inhibitor).[42,47] In addition, there has been a lot of interest in the development of pyridine scaffolds for the treatment of AD.[48,49]

Thiazoles are another class of nitrogen heteroaromatics that are prominently studied. These possess a wide range of pharmacological properties, including antibacterial, antimicrobial, and anticancer activities.[50–53] Apart from these properties, thiazoles have been researched for their cholinesterase inhibitory properties.[54–58] It has been indicated in varied studies that compounds including a thiazole ring are effective against neurodegenerative disorders due to low cholinergic neurotransmitter levels.[59–61]

Based on the above information, we designed and synthesized a series of triheterocycles containing pyridine, thiazole, and 1,3,4-oxadiazole rings, then tested against cholinesterase inhibition activity and evaluated their biological activity via molecular docking and molecular dynamic simulation (MDS) studies.

2 | RESULT AND DISCUSSION

2.1 | Chemistry

The synthesis of the compounds was carried out as outlined in Scheme 1. Ethyl 2-(pyridin-3/4-yl)thiazole-4-carboxylate (**1a,b**) and 2-(pyridin-3/4-yl) thiazole-4-carbohydrazide (**2a,b**) were prepared by literature methods.[53,62–65] Intramolecular cyclization of **2a,b** with carbon disulfide under basic conditions resulted in 5-(2-(pyridin-3/4-yl)thiazol-4-yl)1,3,4-oxadiazol-2(3*H*)-thiones **3a,b**. Then treatment of **3a,b** with substituted benzyl bromides afforded the 2,5-disubstituted-1,3,4-oxadiazoles in 51%–93% yield. The structure of final compounds (**4a-h**, **5a-h**) was confirmed by using fourier transform infrared spectroscopy (FT-IR), ^{1}H NMR, ^{13}C NMR, and MS spectral methods.

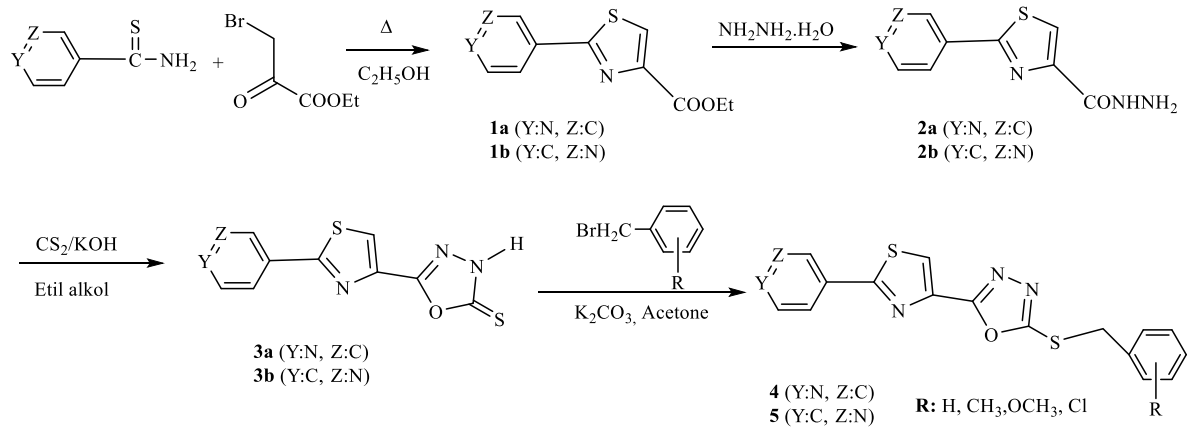

Compound	R	Compound	R
4a	H	5a	H
4b	2-CH_3	5b	2-CH_3
4c	3-CH_3	5c	3-CH_3
4d	4-CH_3	5d	4-CH_3
4e	2-Cl	5e	2-Cl
4f	3-Cl	5f	3-Cl
4g	4-Cl	5g	4-Cl
4h	3-OCH_3	5h	3-OCH_3

SCHEME 1 Synthesis of the 2,5-disubstituted-1,3,4-oxadiazoles **4a-h** and **5a-h**

The structure of key intermediate oxadiazole thione **3a,b** was confirmed by its spectroscopic data. The infrared spectroscopy (IR) spectrum of compounds **3a** and **3b** showed absorption bands, respectively, at 3393 and 3418 cm^{-1} corresponding to the cyclic NH group. The absorption bands due to C=N were observed at 1630 cm^{-1} for **3a** and 1655 cm^{-1} for **3b**. Additionally, the C=S and C–O–C stretching vibrations were absorbed in about 1372 and 1075 cm^{-1}, respectively. Each absorption band is structural evidence for the 1,3,4-oxadiazole-2(3*H*)-thiones. The absence of absorption by hydrazide carbonyl in the region 1760–1705 cm^{-1} indicated the cyclization of the corresponding acid hydrazide. In addition, the absence of the thiol SH absorption band at 2560–2550 cm^{-1} in the IR spectrum and the presence of the C=S absorption band at 1372 cm^{-1} showed that it is in the thione form. In the literature, it is stated that 5-substituted-1,3,4-oxadiazol-2(3*H*)-thiones exist in thione and thiol tautomeric forms. It has been calculated that the thione form is more stable than the thiol form at 9.616 kcal/mol in the gas phase and 12.12 kcal/mol in an aqueous solution, and it is stated in the literature that these results are supported by the spectroscopic data (UV-Vis and IR). The observation of absorption bands supporting the thione form in the IR spectra of the **3a** and **3b** is in accordance with the literature.[60]

The ^{1}H NMR spectrum of compound **3a** displayed peaks, a singlet at 10.11 ppm, indicating the presence of an NH proton of oxadiazole moiety, and a singlet at 8.73 ppm, indicating the presence of a thiazole group. The pyridyl protons resonated in the region 7.96–8.78 ppm. Similarly, compound **3b** showed a singlet at 9.28 ppm for NH (oxadiazole) and the singlet at 8.68 ppm was seen as thiazole proton. The pyridyl protons appeared in the range of 7.56–9.20 ppm.

The formation of final compounds **4a-h** and **5a-h** was confirmed by characteristic IR spectrum absorption bands in the range of 3150–2900, 1090–1066, and 733–696 cm^{-1} corresponding to C=N stretching bands, C–O–C stretching bands for heterocyclic compounds (1,3,4-oxadiazole), and C–S stretching bands, respectively. Singlet peaks at 2.25–2.41, 3.64–3.69, 4.49–4.68, and 8.62–9.22 ppm in ^{1}H NMR were due to $-CH_3$ in phenyl group, $-OCH_3$ in phenyl group, $-S-CH_2-$, and thiazole-H, respectively. The aromatic ring protons were observed at 6.76–8.42 ppm and the *J* value was found to be in accordance with the substitution pattern on the phenyl ring. The pyridine ring protons were observed at 7.94–9.22 ppm. Typical chemical shifts of ^{13}C NMR spectra at around 160.059–167.172, 113.813–161.556, 121.770–161.768, and 120.858–152.207 ppm indicated the presence of the 1,3,4-oxadiazole, phenyl, thiazole, and pyridine moieties, while peaks around 19.285–21.444, 55.448, and 34.466–38.184 ppm confirmed the presence of $-CH_3$, $-OCH_3$, and $-SCH_2-$, respectively. When the ^{13}C-NMR spectrum of all synthesized compounds is examined, the absence of the characteristic C=S peak seen at 176.3 ppm in the synthesized compounds and the signals of $S-CH_2$ carbon atoms in the range of 34.466–38.184 ppm constitute strong evidence for the formation of S substituted products (for more details evaluate the Section 4 and the Supporting Information).

The mass spectra of **4a-h** and **5a-h** revealed that observed molecular ion peaks were in agreement with the molecular weight of the respective compound.

2.2 | Anticholinesterase activity

The anticholinesterase activity of the compounds was carried out on AChE and BChE enzymes at 10^{-3}M and 10^{-4} M concentrations. The results are given as inhibition percentages in Table 1 and Figure 1. The half-maximal inhibition concentration (IC_{50}) values comparable to the standard drugs donepezil and tacrine were achieved for some compounds. Compounds **4a**, **4 h**, **5a**, **5d**, and **5e** showed greater than 90% percent inhibition against AChE at 10^{-3} μM concentration. The same compounds exhibited more than 85% inhibition at 10^{-4} M concentration. The compounds **5e**, **4a**, and **5d** showed prominent anti-AChE activity that IC_{50} values were determined as 0.023, 0.026, and 0.029 μM for compounds **5e**, **4a**, and **5d**, respectively, whereas the IC_{50} value of donepezil was identified as 0.021 μM. Moreover, **4 h** and **5a** displayed high AChE inhibition with IC_{50} values of 0.033 and 0.037 μM. When all compounds were evaluated, inhibition of over 77% against AChE was observed at 10^{-3} M concentration. The IC_{50} values of the remaining compounds were determined to be >100 μM against AChE. When the effects of the compounds on BChE were evaluated, it was observed that they were inhibited within the range of 31.5%–47.1% at 10^{-3} M concentration. This numerical range was decreased to 25.6%–33.8% at 10^{-4} M concentration whereas the inhibition percentage of tacrine was found to be over 95% at these concentrations. The IC_{50} values of all compounds were determined to be >1000 μM against BChE.

2.3 | Molecular docking studies

After determination of the active compounds (**4a**, **4 h**, **5a**, **5d**, and **5e**) against cholinesterase enzymes, our research group evaluated the interacted residues of the AChE, and also their interaction types. The obtained 2D and 3D poses are displayed in Figures 2–4, respectively.

First of all, the docking results have indicated that independently of the pyridine ring, nonsubstituted phenyl rings settle down in a different position than other substitutions into the active pocket, which causes them to move away from Trp286 (see Figure 4). Moreover, these two compounds (**4a** and **5a**) seem to have the same interactions, but compound **5a** has π–π interaction with Tyr341 instead of Trp286 residue, thus, as expected compound **4a** is more active than compound **5a**. In addition, the 3-methoxyphenyl group (**4h**) decreased the inhibitory activity of the core structure because of the lack of important interaction with the CAS (His447, one of the catalytic triad) site of the enzyme. On the other hand, 2-chloro (**5e**) and 4-methyl (**5d**) groups increased the inhibitory activity, as well 2-chloro (**5e**) group interacted with Glh202 as an extra, thus, its activity was more powerful than 4-methyl (**5d**). The fact that 4-benzylpiperidine moiety of donepezil interacts with Trp86 via π–π or π–cation, and the indanone moiety interacts with Trp286 via the same force, it suggests that these amino acids are essential residues in terms of inhibitory activity. Besides that, Phe295 (H-bond) and Glh202 (halogen/H-bonds) amino acids are also the other important residues for AChE inhibition. The most active compound **5e** interacted like

TABLE 1 % Inhibition and IC_{50} values of the synthesized compounds, donepezil, and tacrine against AChE and BChE (n = 4 replicates)

Compounds	Human AChE % inhibition[a]		Human AChE IC_{50} (μM)	Human BChE % inhibition[a]		Human BChE IC_{50} (μM)
	10^{-3} M	10^{-4} M		10^{-3} M	10^{-4} M	
4a	95.3±1.4	90.7±1.3	0.026±0.001	38.7±0.8	30.6±0.7	>1000
4b	81.6±1.1	45.6±0.8	>100	40.9±0.9	28.4±0.6	>1000
4c	85.7±1.3	42.4±0.9	>100	42.0±0.8	31.1±0.7	>1000
4d	86.8±1.5	41.8±0.7	>100	36.1±0.7	32.8±0.8	>1000
4e	80.0±1.4	40.1±0.8	>100	31.5±0.8	27.0±0.6	>1000
4f	78.2±0.9	48.2±1.0	>100	39.3±0.9	30.9±0.7	>1000
4g	88.4±1.0	46.0±0.9	>100	43.4±0.8	27.7±0.7	>1000
4h	93.8±1.6	87.3±1.3	0.033±0.001	45.6±0.9	28.3±0.8	>1000
5a	94.9±2.0	85.1±1.4	0.037±0.001	30.7±0.8	24.0±0.6	>1000
5b	87.6±1.3	45.4±1.1	>100	38.0±0.7	30.2±0.7	>1000
5c	82.9±1.6	43.8±0.9	>100	34.5±0.8	26.4±0.6	>1000
5d	94.6±1.6	89.1±1.3	0.029±0.001	44.9±0.9	28.6±0.7	>1000
5e	96.2±1.1	92.5±1.4	0.023±0.001	47.1±0.9	31.1±0.8	>1000
5f	86.1±1.2	40.9±0.8	>100	41.2±0.8	33.5±0.8	>1000
5g	77.0±1.5	47.3±1.0	>100	40.6±0.8	26.2±0.6	>1000
5h	83.5±1.1	46.4±0.9	>100	38.5±0.7	25.6±0.7	>1000
Donepezil	99.2±2.1	97.4±1.8	0.021±0.001	-	-	-
Tacrine	-	-	-	98.2±1.8	95.4±1.3	0.0064±0.0-002

[a]Human acetylcholinesterase (CAS No: 9000-81-1) and human butyrylcholinesterase (CAS No: 9001-08-5).

donepezil. Finally, we suggest that even if the active compounds showed very close activity potential, compound **5e** is more active than the others because of the essential interactions with the important residues since its shape fits well.

The presence of aromatic H-bonds between the compounds (**4h**, **5d**, and **5e**) and the Glh202 amino acid points out the AChE's selectivity. The bond strength of interaction with Glh202 can cause differences in inhibitory activity, therefore, this amino acid is another important residue. In fact, the most active compound **5e** formed additionally a halogen bond with Glh202. The molecular docking study was found in harmony with the in vitro enzyme study. All compounds fit well into the active pocket of the enzyme and interacted with it, thus, the docking study explained the binding mode of the active compounds.

2.4 | Results of MDS

After all, although the docking studies explained the behavior of the ligand–enzyme complex together and separately since it is applied not considering the time (the 4th dimension) and the enzyme is usually kept rigid, it is not fully imitated in the biological system. In addition to this, understanding the effects of environmental factors on the complex is another important issue. Because of mentioned reasons, we also performed the MDS for the most active compound (**5e**).

First, the system stability was checked (in Figure 5). According to the Rg plot (which informed about the compactness of the complex), between 5.10 and 5.30 ns, the system was unstable, but after that, there was no fluctuation in this plot. Root-mean-square deviation (RMSD) value of protein is indicative of stability,[66] it was calculated between 1 and 3 Å during the entire simulation. Root-mean-squared fluctuation (RMSF) plot has three regions, which are red for α-helix, blue for β-strand, and white for the loop. The helix and strand residues usually are stable and have minimum fluctuation, on the other hand, loop residues usually show big fluctuation. According to our results, amino acids numbered between 286 and 299 are a member of the loop region and showed minimal fluctuation than expected. It is probably related that there were some interacted amino acids in this region, resulting in increasing the system stability. In conclusion, the stability of the **5e**-AChE complex was protected during the simulation.

According to interaction results obtained from MDS (see Figure 6), there are three direct interactions (H-bond, halogen bond, and π–π stacking). Additionally, the water-mediated H-bonds (the interactions fraction-residue in Figure 6), and aromatic H-bonds (see the video in the Supporting Information) are observed. Although the halogen bond was formed between Glh202 and ligand according to the docking study, the halogen bond was observed occasionally, which means that this bond was not as influential to activity as not expected. Moreover, it was mostly formed with Tyr337 and His447 (see the video). Therefore, even if the

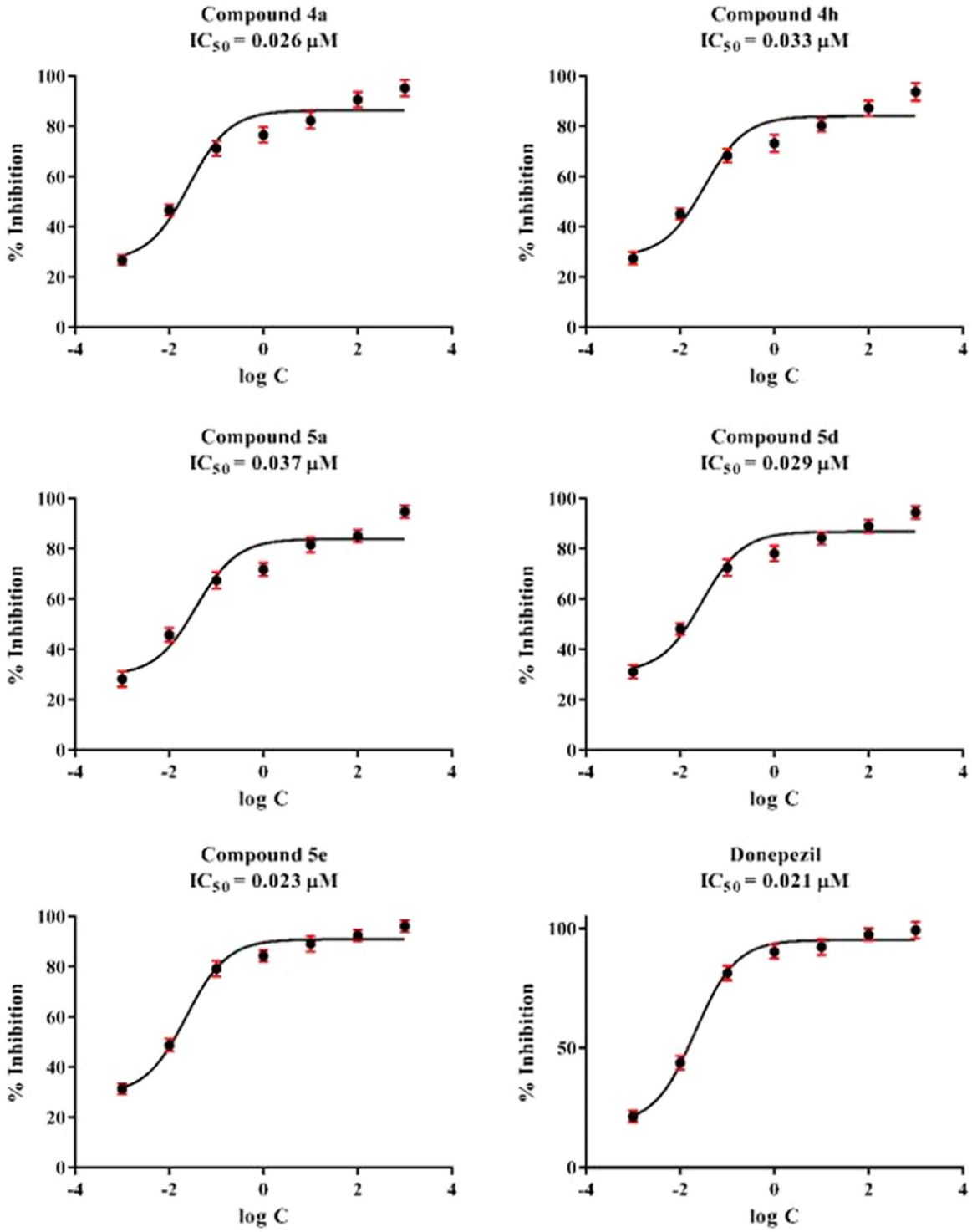

FIGURE 1 IC_{50} graphs of compounds **4a**, **4h**, **5a**, **5d**, **5e**, and donepezil on the acetylcholinesterase (AChE) enzyme. The graphs are formed using GraphPad Prism Version 6 via regression analyses.

halogen bond may increase the activity, the major part is not related to the direct effect of this substitution. On the other hand, the instability between 5.10 and 5.30 ns may be caused by the relation between ligand and Tyr124 amino acid. Instability of the system was detected at the same time as the lack of interactions between ligand and Tyr124 amino acid. Some interactions were seen frequently, which were made with Tyr72, Trp86, Tyr124, Trp286, Phe295, Tyr337, and Tyr341 amino acids. However, the most contact strength interaction is formed between Trp86 (96%). And also, there was one important water molecule that mediated the H-bond between Tyr72 and nitrogen of the oxadiazole ring. As a result, the MDS study clarified and explained the importance of chlorine substitution, system stability, and the important residues for the activity.

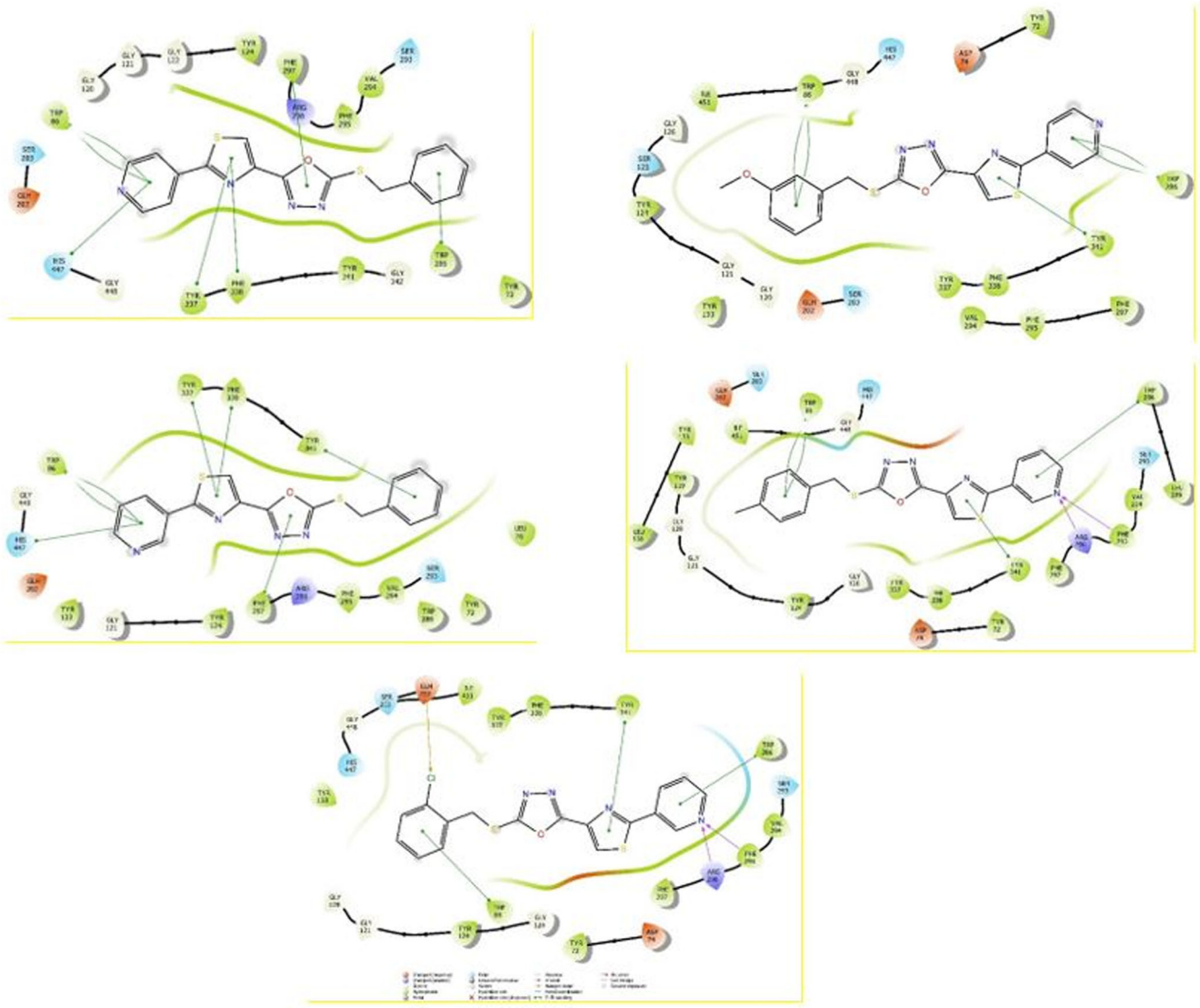

FIGURE 2 2D interaction diagram of the active compounds **4a**, **4h**, **5a**, **5d**, and **5e**, respectively, on acetylcholinesterase (AChE) (PDBID: 4EY7) binding pocket. *Compounds put in order from left to right and top to bottom considering their name.

2.5 | Prediction of pharmacokinetic properties

Sixteen final compounds were evaluated in SwissADME free software to predict absorption, distribution, metabolism, and excretion (ADME), pharmacokinetic properties, and drug-likeness properties and the results are displayed in Table 2. Number of H-bond acceptors (NBA), number of H-bond donors (NBD), topological polar surface area (TPSA), partition coefficient (Log P), gastrointestinal absorption (GI) level, and level of crossing the blood–brain barrier (BBB) of the compounds were calculated, virtually. According to Lipinski's rule of five,[67] an oral drug should have a molecular weight of fewer than 500 daltons, log P less than 5.0, ≤10 hydrogen bond acceptor, and ≤5 hydrogen bond donor for fair solubility and permeability. All compounds satisfy this rule that compounds have high GI, except compounds including chloro and methoxy substituents. None of the compounds exhibited BBB permeability although relatively high log P values were detected between 3.61 and 4.19. TPSA, which is described as the sum of all polar atoms or molecules surfaces over the compounds, was calculated between 118.24 and 127.47. Furthermore, compound **5e** has differences because of its Log P value (4.14).

3 | CONCLUSION

In summary, we have synthesized a series of S-substituted 1,3,4-oxadiazoles, including pyridine and thiazole heterocycles. The bioactivity data of 2,5-disubstituted-1,3,4-oxadiazoles **4a-h** and **5a-h** and molecular docking studies concluded that compounds **4a**, **4 h**, **5a**, **5d**, and **5e** showed good inhibitory activity against AChE. Among them, the most potent compound **5e** showed an IC_{50} value of 0.023 μM against AChE. Molecular docking studies display the favorable interactions of compound **5e** with Trp86 in the AChE active site, which is obligatory for inhibition activity. Moreover, MDS studies indicated the stability of this bond strength with Trp86, and it is calculated as 96%.

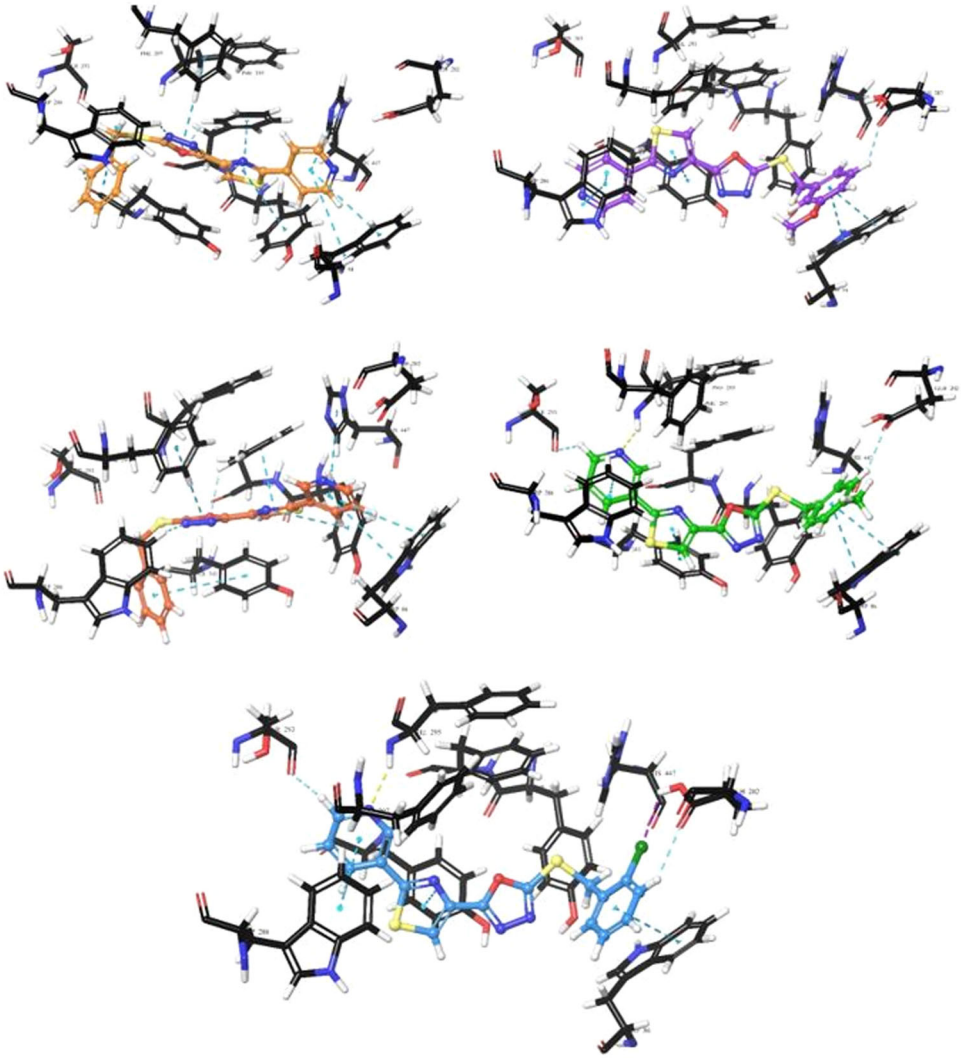

FIGURE 3 3D poses of the active compound **4a**, **4h**, **5a**, **5d**, and **5e** at acetylcholinesterase (AChE) (PDBID: 4EY7) pocket. Compounds are put in order from left to right and top to bottom considering their name.

4 | EXPERIMENTAL

4.1 | Chemistry

4.1.1 | General

All chemicals were purchased from Aldrich Chemical Co., Merck, and Alfa Aesar. The melting points were determined by Gallenkamp digital melting point apparatus and were uncorrected. The purity of the compounds was checked by thin-layer chromatography on silica gel-coated aluminum sheets (Merck, 1.005554, silica gel HF254–361, Type 60, 0.25 mm). The IR spectra (KBr) were recorded on a Bruker FT-IR spectrometer,^{1}H-NMR, and ^{13}C NMR spectra were obtained by a JEOL ECZ500R (11.75 Tesla) spectrometer in DMSO-*d6*. All the chemical shifts were recorded as δ (ppm) values. High-resolution mass spectrometric (HRMS) analyses were performed using an time-of-flight mass spectrometry system (Shimadzu).

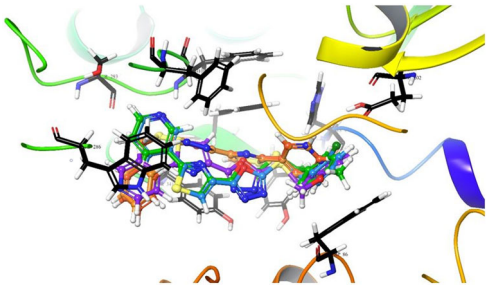

FIGURE 4 3D superimposition of the active compounds **4a** (orange carbons), **4h** (faded-orange carbons), **5a** (purple carbons), **5d** (green carbons), and **5e** (blue carbons) at the acetylcholinesterase (AChE) pocket (PDBID: 4EY7).

The original ^{1}H and ^{13}C NMR spectra of the investigated compounds (**4a-h** and **5a-h**) are given as a Supporting Information file. The InChI codes of the investigated compounds, together with some biological activity data, are also provided as Supporting Information.

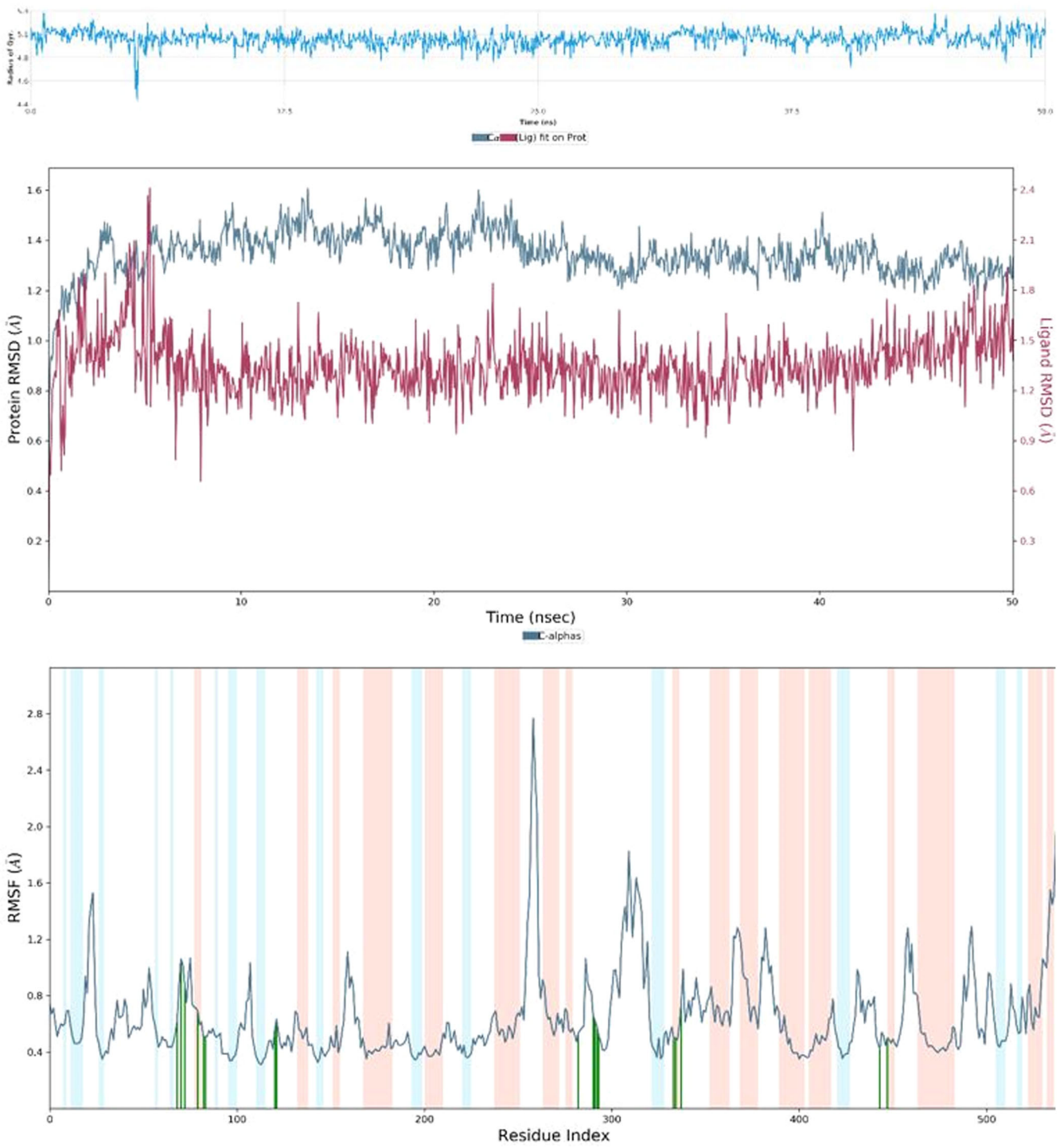

FIGURE 5 The stability plots of Rg, RMSD, and RMSF values for the **5e**-acetylcholinesterase (AChE) complex, respectively

4.1.2 | Synthesis of ethyl 2-(pyridin-3/4-yl)thiazole-4-carboxylate (**1a,b**)

Pyridine-3/4-thiocarboxamide (11.02 g, 79.7 mmol) was dissolved in 200 ml of ethanol. Ethyl bromopyruvate (12 ml, 95.64 mmol) was added to this solution and this mixture was refluxed at 80°C for 8 h. After the reaction was brought to room temperature, the collected precipitate was filtered and then crystallized from ethanol.[51,60–63] Yield: 82% (**1a**), 71% (**1b**); mp: 219–221°C (**1a**), 200–202°C (**1b**).

4.1.3 | Synthesis of 2-(pyridin-3/4-yl)thiazole-4-carbohydrazide (**2a,b**)

Ethyl 2-(pyridin-3/4-yl)thiazole-4-carboxylate (1) (13.14 g, 56.10 mmol) and hydrazine hydrate (6.82 ml, 140 mmol) were stirred in ethanol at room temperature for 12 h. The collected precipitate was filtered and washed in cold methanol and dried.[53,62–65] Yield: 74% (**2a**), 94% (**2b**); mp: 193–198°C (**2a**), 158–161°C (**2b**).

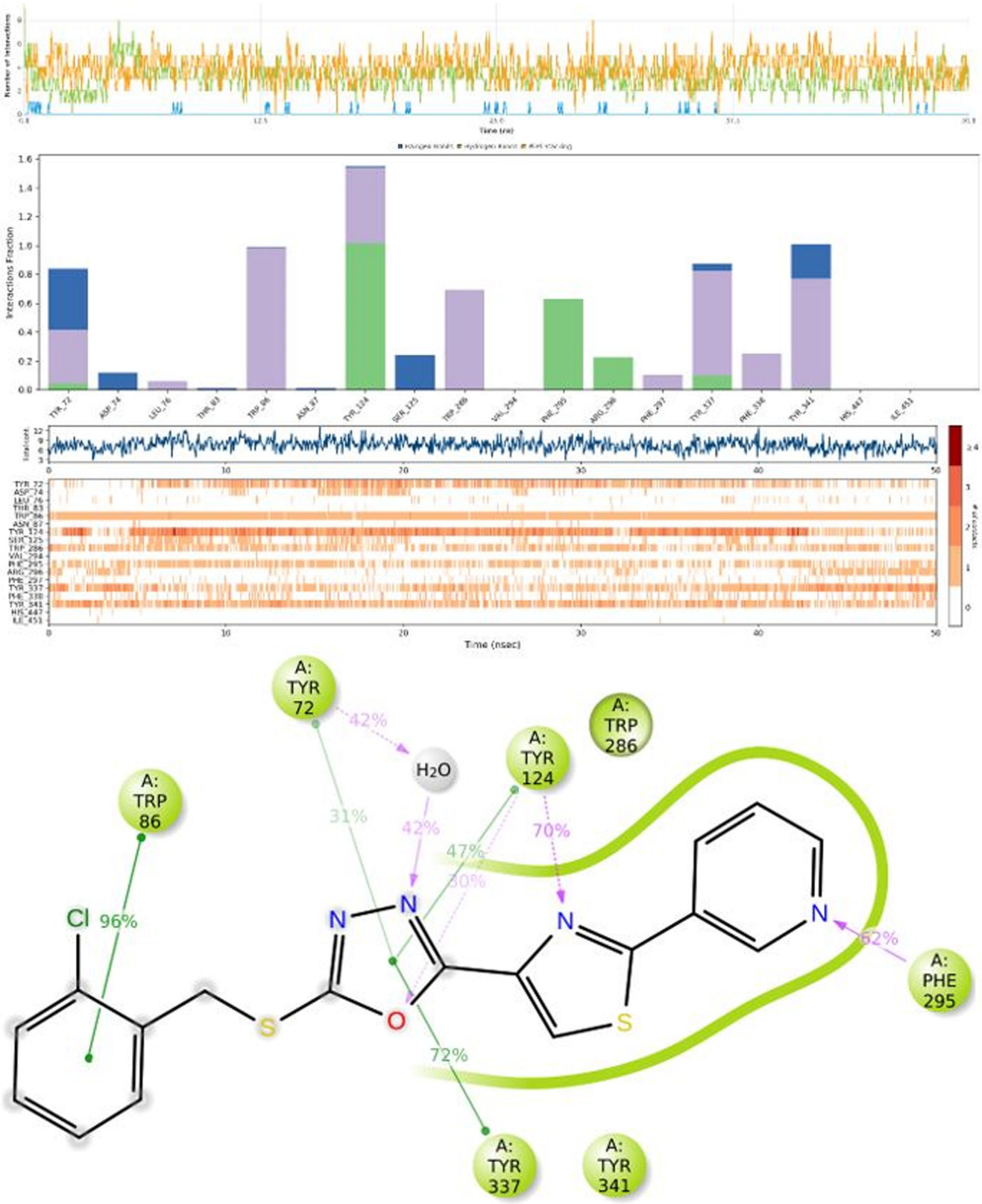

FIGURE 6 The plots of the number of interactions and types-time, the interactions fraction-residue, the residue-time, and the diagram of contact strength (cutoff = 30%) as the 2D pose of the **5e**-acetylcholinesterase (AChE) complex, respectively

TABLE 2 ADME parameters

Comp.	M.F.	M.W.	NBA	NBD	TPSA (Å²)	Log P	GI abs.	BBB perm.
4a	$C_{17}H_{12}N_4OS_2$	352.43	5	0	118.24	3.65	High	No
4b	$C_{18}H_{14}N_4OS_2$	366.46	5	0	118.24	3.93	High	No
4c	$C_{18}H_{14}N_4OS_2$	366.46	5	0	118.24	4.00	High	No
4d	$C_{18}H_{14}N_4OS_2$	366.46	5	0	118.24	3.97	High	No
4e	$C_{17}H_{11}ClN_4OS_2$	386.88	5	0	118.24	4.18	Low	No
4f	$C_{17}H_{11}ClN_4OS_2$	386.88	5	0	118.24	4.15	Low	No
4g	$C_{17}H_{11}ClN_4OS_2$	386.88	5	0	118.24	4.19	Low	No
4h	$C_{18}H_{14}N_4O_2S_2$	382.46	6	0	127.47	3.61	Low	No
5a	$C_{17}H_{12}N_4OS_2$	352.43	5	0	118.24	3.63	High	No
5b	$C_{18}H_{14}N_4OS_2$	366.46	5	0	118.24	3.93	High	No
5c	$C_{18}H_{14}N_4OS_2$	366.46	5	0	118.24	3.98	High	No
5d	$C_{18}H_{14}N_4OS_2$	366.46	5	0	118.24	3.99	High	No
5e	$C_{17}H_{11}ClN_4OS_2$	386.88	5	0	118.24	4.14	Low	No
5f	$C_{17}H_{11}ClN_4OS_2$	386.88	5	0	118.24	4.16	Low	No
5g	$C_{17}H_{11}ClN_4OS_2$	386.88	5	0	118.24	4.19	Low	No
5h	$C_{18}H_{14}N_4O_2S_2$	382.46	6	0	127.47	3.61	Low	No

4.1.4 | Synthesis of 5-[2-(pyridin-4-yl)thiazol-4-yl]-1,3,4-oxadiazol-2(3*H*)-thione (**3a**)

2-(Pyridin-4-yl) thiazole-4-carbohydrazide (1.76 g, 8 mmol) was dissolved in 30 ml of ethanol. To this solution, CS_2 (1 ml, 16.8 mmol) and KOH (0.538 g, 9.6 mmol) dissolved in 7 ml of H_2O were added and the mixture was refluxed at 200°C for 9 h and then cooled to room temperature. The reaction mixture was poured into ice water and acidified with dilute HCl till the formation of white precipitate was separated. The substance was completely precipitated by keeping it in the refrigerator for a night. The precipitate formed was achieved by filtration. The separated solid was washed with cold water and dried. The completion of the reaction was monitored on thin layer chromatography (TLC) using chloroform/methanol (6:4) as the mobile phase.[65]

Yield: 84%; mp: 263–265°C; IR υ_{max}(cm^{-1}): 3391 (N–H stretching band), 3111–2950 (aromatic C–H stretching band), 1630 (C═N stretching band), 1599–1453 (aromatic C═C stretching band, NH bending), 1372 (C═S stretching band), 1075 (C–O–C stretching band); ^{1}H NMR (500 MHz, DMSO-d_6), δ: 10,11 (s, 1H, NH), 8.78–8.76 (d, J = 6.42 Hz, 2H, pyridine-H), 8.73 (s,1H, thiazole-H), 7.98–7.96 (dd, J = 4.50, J = 1.69 Hz 2H, pyridine-H).

4.1.5 | Synthesis of 5-[(2-(pyridin-3-yl)thiazol-4-yl]-1,3,4-oxadiazol-2(3*H*)-thione (**3b**)

2-(Pyridin-3-yl) thiazole-4-carbohydrazide (3.30 g, 15.02 mmol) was dissolved in 20 ml of ethanol. To this solution, CS_2 (2.26 ml, 37.55 mmol) and KOH (1.05 g, 18.78 mmol) dissolved in 7 ml of H_2O were added and refluxed at 200°C for 9 h and then cooled to room temperature. The reaction mixture was poured into ice water and acidified with dilute HCl till the formation of white precipitate was separated. The substance was completely precipitated by keeping it in the refrigerator for a night. The precipitate formed was filtered. The separated solid was washed with cold water and dried. The completion of the reaction was monitored on TLC using chloroform/methanol (6:4) as the mobile phase.[65]

Yield: 37%; mp: 262–264°C; IR υ_{max} (cm^{-1}): 3418 (N–H stretching band), 3086–2950 (aromatic C–H stretching band), 1655 (C═N stretching band), 1620–1453 (aromatic C═C stretching band, NH bending), 1372 (C═S stretching band), 1075 (C–O–C stretching band). ^{1}H NMR (500 MHz, DMSO-d_6), δ: 9.28 (d, J = 2.17 Hz, 1H, NH), 9.20 (d, J = 2.3 Hz, 1H, pyridine- H), 8.74 (dd, J = 4.9, 1.6 Hz, 1H, pyridine-H), 8.68 (s, 1H, thiazole-H), 8.46–8.34 (dd, J = 8.15, 6.09 Hz, 1H, pyridine-H), 7.62–7.56 (dd, J = 4.74 Hz, J = 3.23 Hz, 1H, pyridine-H).

4.1.6 | General procedure for the synthesis of 2,5-disubstituted-1,3,4-oxadiazoles (**4a-4h**)

5-[2-(Pyridin-4-yl) thiazol-4-yl]-1,3,4-oxadiazol-2(3*H*)-thione (**3a**) (0.1 g, 0.38 mmol) and appropriate benzyl bromide derivatives (0.38 mmol), and potassium carbonate were dissolved in acetone and stirred at room temperature for 4–18 h. The completion of the reaction was monitored on TLC using chloroform/methanol (8:4) as the mobile phase. Then, acetone was concentrated in a vacuum and the precipitate was treated with water, filtered, and dried. The obtained product was washed with ethanol and dried.[65]

*2-(Benzylthio)-5-[2-(pyridin-4-yl)thiazol-4-yl]-1,3,4-oxadiazole (**4a**)*

Yield: 85%; mp: 154–156°C; IR $\upsilon_{max}(cm^{-1})$: 3086–2900 (aromatic C–H stretching band), 1632 (C=N stretching band), 1594–1472 (aromatic C=C stretching band), 1084 (C–O–C stretching band), 1171, 989, 920 (aromatic C–H in-plane bending bands), 812, 762 (aromatic C–H out-of-plane bending), 702 (C–S stretching band). ^{1}H NMR (500 MHz, DMSO-d_6), δ: 8.78–8.76 (m, 3H, pyridine-H, thiazole-H), 7.99 (dd, J = 4.43 Hz, J = 1.69 Hz 2H, pyridine-H), 7.51 (d, J = 6.9 Hz, 1H, Ar-H), 7.42–7.26 (m, 4H, Ar-H), 4.62 (s, 2H, S-CH_2). ^{13}C NMR (125 MHz, DMSO-d_6), δ: 35, 120.848, 126.588, 128.374, 129.142, 129.622, 129.890, 136.907, 139.124, 140.468, 151.459, 161.460, 164.042, 167.162. HRMS (m/z): $[M+1]^+$: for $C_{17}H_{12}N_4OS_2$ calculated: 353.0525, found: 353.0518.

*2-(2-Methylbenzylthio)-5-[2-(pyridin-4-yl)thiazol-4-yl]-1,3,4-oxadiazole (**4b**)*

Yield: 85%; mp: 134–137°C; IR $\upsilon_{max}(cm^{-1})$: 3115–2900 (aromatic C–H stretching band), 2861 (aliphatic C–H stretching band), 1640 (C=N stretching band), 1593–1478 (aromatic C=C stretching band), 1077 (C–O–C stretching band), 1165, 993, 955 (aromatic C–H in-plane bending bands), 758 (aromatic C–H out-of-plane bending), 723 (C–S stretching band). ^{1}H NMR (500 MHz, DMSO-d_6), δ: 8.78–8.76 (m, 3H, pyridine-H, thiazole H), 7.98 (dd, J = 4.5 Hz, J = 1.77Hz, 2H pyridine-H), 7.43 (d, J = 7.13 Hz, 1H, Ar- H), 7.24–7.15 (m, 3H, Ar-H), 4.62 (s, 2H, S-CH_2), 2.41 (s, 3H, CH_3). ^{13}C NMR (125 MHz, DMSO-d_6), δ: 19.304, 35.094, 120.868, 126.694, 128.844, 130.639, 131.052, 134.123, 137.435, 139.134, 140.458, 151.449, 161.480, 163.860, 167.152. HRMS (m/z): $[M+1]^+$ for $C_{18}H_{14}N_4OS_2$ calculated: 367.0682, found: 367.0689.

*2-(3-Methylbenzylthio)-5-[2-(pyridin-4-yl)thiazol-4-yl]-1,3,4-oxadiazole (**4c**)*

Yield: 72%; mp: 147–150°C; IR $\upsilon_{max}(cm^{-1})$: 3111–2900 (aromatic C–H stretching band), 2860 (aliphatic C–H stretching band), 1678 (C=N stretching band), 1595–1470 (aromatic C=C stretching band), 1084 (C–O–C stretching band), 1165, 999, 948, 881 (aromatic C–H in-plane bending bands), 821, 787 (aromatic C–H out-of-plane bending bands), 708 (C–S stretching band). ^{1}H NMR (500 MHz, DMSO-d_6), δ: 8.79–8.62 (m, 3H, pyridine-H, thiazole-H), 7.98 (dd, J = 4.46 Hz J = 1.71 Hz 2H pyridine-H), 7.34–6.95 (m, 4H Ar-H), 4.56 (s, 2H, S-CH_2), 2.27 (s, 3H, CH_3). ^{13}C NMR (125 MHz, DMSO-d_6), δ: 21.444, 36.476, 120.829, 126.560, 126.713, 129.046, 130.197, 136.686, 138.328, 139.076, 140.449, 151.449, 161.412, 164.062, 167.133. HRMS (m/z): $[M+1]^+$ for $C_{18}H_{14}N_4OS_2$ calculated: 367.0682, found: 367.0679.

*2-(4-Methylbenzylthio)-5-[2-(pyridin-4-yl)thiazol-4-yl]-1,3,4-oxadiazole (**4d**)*

Yield: 88%; mp: 166–170°C; IR $\upsilon_{max}(cm^{-1})$: 3121–2900 (aromatic C–H stretching band), 2862 (aliphatic C–H stretching band), 1692 (C=N stretching band), 1593–1478 (aromatic C=C stretching band), 1079 (C–O–C stretching band), 1167, 995, 955 (aromatic C–H in-plane bending bands), 824 (aromatic C–H out-of-plane bending bands), 719 (C–S stretching band). ^{1}H NMR (500 MHz, DMSO-d_6), δ: 8.78–8.76 (m, 3H, pyridine-H, thiazole-H), 7.98 (dd, J = 4.34Hz J = 1.85 Hz, 2H, pyridine-H), 7.38 (d, J = 8.053 Hz, 2H, Ar-H), 7.16 (d, J = 7.9Hz, 2H, Ar-H), 4.56 (s, 2H, S-CH_2), 2.27 (s, 3H, CH_3). ^{13}C NMR (125 MHz, DMSO-d_6), δ: 21.243, 36.332, 120.868, 126.627, 129.574, 129.698, 129.814, 133.768, 137.713, 139.134, 140.458, 151.449, 161.422, 164.081, 167.143. HRMS (m/z): $[M+1]^+$ for $C_{18}H_{14}N_4OS_2$ calculated: 367.0682, found: 367.0674.

*2-(2-Chlorobenzylthio)-5-[2-(pyridin-4-yl)thiazol-4-yl]-1,3,4-oxadiazole (**4e**)*

Yield: 72%; mp: 156–158°C; IR $\upsilon_{max}(cm^{-1})$: 3115–2900 (aromatic C–H stretching band), 1674 (C=N stretching band), 1597–1483 (aromatic C=C stretching band), 1090 (C–O–C stretching band), 1175, 1053, 1035 (aromatic C–H in-plane bending bands), 754 (aromatic C–H out-of-plane bending bands), 733 (C–S stretching band). ^{1}H NMR (125 MHz, DMSO-d_6), δ: 8.73–8.77 (m, 3H, pyridine-H, thiazole-H), 7.98 (dd, J = 4.53 Hz 1.83 Hz, 2H, pyridine-H), 7.64 (dd, J = 7.2, 2.2 Hz, 1H, Ar-H), 7.53–7.47 (dd, 1H, J = 7.5 Hz, J = 1.96 Hz, Ar-H), 7.35 (m, 2H, Ar-H), 4.67 (s, 2H,S-CH_2). ^{13}C NMR (125 MHz, DMSO-d_6), δ: 34.892, 120.877, 126.790, 128.057, 130.188, 130.610, 132.204, 133.874, 134.239, 139.143, 140.430, 151.449, 161.681, 163.524, 167.172. HRMS (m/z): $[M+1]^+$ for $C_{17}H_{11}N_4OS_2Cl$ calculated: 387.0136, found: 387.0138.

*2-(3-Chlorobenzylthio)-5-[2-(pyridin-4-yl)thiazol-4-yl]-1,3,4-oxadiazole (**4f**)*

Yield: 63%; mp: 168–169°C; IR $\upsilon_{max}(cm^{-1})$: 3092–2900 (aromatic C–H stretching band), 1623 (C=N stretching band), 1595–1470 (aromatic C=C stretching band), 1173, 1010, 993, 881 (aromatic C–H in-plane bending bands), 1082 (C–O–C stretching band), 822, 795 (aromatic C–H out-of-plane bending bands), 716 (C–S stretching band). ^{1}H NMR (500 MHz, DMSO-d_6), δ: 8.75–8.68 (m, 3H, pyridine-H, thiazole-H), 7.94 (dd, J = 4.52 Hz, J = 1.75 Hz, 2H, pyridine-H), 7.56 (t, J = 1.9 Hz, 1H, Ar-H), 7.44–7.29 (m, 3H, Ar-H), 4.55 (s, 2H, S-CH_2). ^{13}C NMR (125 MHz, DMSO-d_6), δ: 35.631, 120.877, 126.675, 128.287, 128.374, 129.497, 130.985, 133.499, 139.134, 139.796, 140.430, 151.420, 161.547, 163.870,167.133. HRMS (m/z): $[M+1]^+$ for $C_{17}H_{11}N_4OS_2Cl$ calculated: 387.0136, found: 387.0136.

*2-(4-Chlorobenzylthio)-5-[2-(pyridin-4-yl)thiazol-4-yl]-1,3,4-oxadiazole (**4g**)*

Yield: 93%; mp: 169–172°C; IR $\upsilon_{max}(cm^{-1})$: 3150–2900 (aromatic C–H stretching band), 1642 (C=N stretching band), 1593–1482 (aromatic C=C stretching band), 1078 (C–O–C stretching band), 1161, 995 (aromatic C–H in-plane bending bands), 821 (aromatic C–H out-of-plane bending bands), 721 (C–S stretching band). ^{1}H NMR (500 MHz, DMSO-d_6), δ: 8.78 (d, J = 1.77 Hz 1H, pyridine-H), 8.77 (d, J =1.7 Hz, 1H, pyridine-H), 8.77 (s, 1H, thiazole-H), 7.98 (dd, J = 4.35 Hz, 1.72 Hz, 2H, pyridine-H, pyridine-H), 7.53 (dd, J = 8.19, 6.28 Hz, 2H, Ar-H), 7.42 (dd, J = 7.98, 6.3 Hz, 2H, Ar-H), 4.60 (s, 2H, S-CH_2). ^{13}C NMR (125 MHz, DMSO-d_6), δ: 35.650, 120.858, 126.665, 129.084, 131.532, 132.962, 136.283, 139.124, 140.430,

151.449, 161.528, 163.889, 167.152. HRMS (*m/z*): $[M+1]^+$ for $C_{17}H_{11}N_4OS_2Cl$ calculated: 387.0136, found: 387.0134.

*2-(3-Methoxybenzylthio)-5-[2-(pyridin-4-yl)thiazol-4-yl]-1,3,4-oxadiazole (**4h**)*

Yield: 90%; mp: 134–137°C; IR $\upsilon_{max}(cm^{-1})$: 3119–2900 (aromatic C–H stretching band), 2837 (aliphatic C–H stretching band), 1635 (C=N stretching band), 1591–1474 (aromatic C=C stretching band), 1161, 1042, 993 (aromatic C–H in-plane bending bands), 1075 (C–O–C stretching band), 823, 781 (aromatic C–H out-of-plane bending bands), 700 (C–S stretching band). ^{1}H NMR (500 MHz, DMSO-d_6), δ: 8.76–8.74 (m, J = 4.7, 1.5 Hz, 3H, pyridine-H, pyridine-H, thiazole-H), 7.96 (dd, J = 4.59Hz J = 1.77 Hz, 2H, pyridine-H, pyridine-H), 7.26–6.83 (m, 4H, Ar-H), 4.54 (s, 2H, S-CH_2), 3.69 (s, 3H, OCH_3). ^{13}C NMR (125 MHz, DMSO-d_6), δ: 36.447, 55.548, 113.822, 115.233, 120.858, 121.770, 126.617, 130.255, 138.376, 139.124, 140.449, 151.411, 159.771, 161.451, 164.052, 167.133. HRMS (*m/z*): $[M+1]^+$ for $C_{18}H_{14}N_4O_2S_2$ calculated: 383.0631, found: 383.0627.

4.1.7 | General procedure for the synthesis of 2,5-disubstituted-1,3,4-oxadiazoles (**5a-5h**)

5-[2-(Pyridin-3-yl) thiazol-4-yl]-1,3,4-oxadiazol-2(3*H*)-thione (**3b**) (0.1 g, 0.38 mmol) and benzyl bromide derivatives (0.38 mmol), and potassium carbonate were dissolved in acetone and stirred at room temperature for 5–12 h. The completion of the reaction was monitored on TLC using chloroform/methanol (8:4) as the mobile phase. Then, acetone was concentrated in a vacuum and the precipitate was treated with water, filtered, and dried. The obtained product was washed with ethanol and dried.[63]

*2-(Benzylthio)-5-[2-(pyridin-3-yl)thiazol-4-yl]-1,3,4-oxadiazole (**5a**)*

Yield: 51%; mp: 142–147°C; IR $\upsilon_{max}(cm^{-1})$: 3065–2900 (aromatic C–H stretching band), 1676 (C=N stretching band), 1588–1472 (aromatic C=C stretching band), 1066 (C–O–C stretching band), 1171, 1020, 981 (aromatic C–H in-plane bending bands), 812,767 (aromatic C–H out-of-plane bending bands), 696 (C–S stretching band). ^{1}H NMR (500 MHz, DMSO-d_6), δ: 9.21 (d, J = 2.3 Hz, 1H, pyridine-H), 8.73 (dd, J = 4.8, 1.6 Hz, 1H, pyridine-H), 8.70 (s, 1H, thiazole-H), 8.40 (dd, J = 8, 2.4 Hz, 1H, pyridine-H), 7.60 (dd, J = 8.4, 4.8 Hz, 1H, pyridine-H), 7.52–7.31 (m, 5H, Ar-H), 4.60 (s, 2H, S-CH_2). ^{13}C NMR (125 MHz, DMSO-d_6), δ: 36.466, 124.937, 125.619, 128.374, 128.652, 129.142, 129.142, 129.910, 134.632, 136.945, 140.123, 147.677, 152.169, 161.547, 163.937, 166.740. HRMS (*m/z*): $[M+1]^+$ for $C_{17}H_{12}N_4OS_2$ calculated: 353.0525, found: 353.0518.

*2-(2-Methylbenzylthio)-5-[2-(pyridin-3-yl)thiazol-4-yl]-1,3,4-oxadiazole (**5b**)*

Yield: 78%; mp: 83–87°C; IR $\upsilon_{max}(cm^{-1})$: 3065–2900 (aromatic C–H stretching band), 2859 (aliphatic C–H stretching band), 1640 (C=N stretching band), 1586–1466 (aromatic C=C stretching band), 1088 (C–O–C stretching band), 1171, 1046, 1023, 982 (aromatic C–H in-plane bending bands), 771 (aromatic C–H out-of-plane bending bands), 727 (C–S stretching band). ^{1}H NMR (500 MHz, DMSO-d_6), δ: 9.22 (d, J = 2.3 Hz, 1H, pyridine-H), 8.74 (dd, J = 4.8, 1.6 Hz, 1H, pyridine-H), 8.72 (s, 1H, thiazole-H), 8.41 (dd, J = 8, 2.4 Hz, 1H, pyridine-H), 7.61 (dd, J = 8, 4.8 Hz, 1H, pyridine-H), 7.43–7.14 (m, 5H, Ar-H), 4.63 (s, 2H, S-CH_2), 2.41 (s, 3H, CH_3). ^{13}C NMR (125 MHz, DMSO-d_6), δ: 19.285, 35.074, 124.947, 125.638, 126.684, 128.633, 128.844, 130.629, 131.042, 134.143, 134.613, 137.425, 140.123, 147.677, 152.188, 161.566, 163.764, 166.759. HRMS (*m/z*): $[M+1]^+$ for $C_{18}H_{14}N_4OS_2$ calculated: 367.0682, found: 367.0673.

*2-(3-Methylbenzylthio)-5-[2-(pyridin-3-yl)thiazol-4-yl]-1,3,4-oxadiazole (**5c**)*

Yield: 54%; mp: 109–111°C; IR $\upsilon_{max}(cm^{-1})$: 3063–2900 (aromatic C–H stretching band), 2859, 2731 (aliphatic C–H stretching band), 1676 (C=N stretching band), 1590–1472 (aromatic C=C stretching band), 1173, 1046, 1017, 982 (aromatic C–H in-plane bending bands), 1088 (C–O–C stretching band), 839, 793 (aromatic C–H out-of-plane bending bands), 700 (C–S stretching band). ^{1}H NMR (500 MHz, DMSO-d_6), δ: 9.18 (d, J = 2.3 Hz, 1H, pyridine-H), 8.71 (dd, J = 4.75, 1,61 Hz 1H, pyridine-H), 8.69 (s, 1H, thiazole-H), 8.38 (dd, J = 8, 2.4 Hz, 1H, pyridine-H), 7.58 (dd, J = 8, 8.4Hz, 1H, pyridine-H), 7.32–7.05 (m, 4H, Ar-H), 4.54 (s, 2H, S-CH_2), 2.25 (s, 3H, CH_3). ^{13}C NMR (125 MHz, DMSO-d_6), δ: 21.435, 38.184, 124.774, 126.300, 126.675, 128.767, 128.911, 128.978, 130.121, 134.555, 136.581, 138.299, 147.782, 150.278, 151.939, 156.536, 160.059, 165.002. HRMS (*m/z*): $[M+1]^+$ for $C_{18}H_{14}N_4OS_2$ calculated: 367.0682, found: 367.0679.

*2-(4-Methylbenzylthio)-5-[2-(pyridin-3-yl)thiazol-4-yl]-1,3,4-oxadiazole (**5d**)*

Yield: 82%; mp: 145–147°C; IR $\upsilon_{max}(cm^{-1})$: 3121–2918 (aromatic C–H stretching band), 2861, 2737 (aliphatic C–H stretching band), 1601 (C=N stretching band), 1570–1476 (aromatic C=C stretching band), 1077 (C–O–C stretching band), 1165, 1046, 984 (aromatic C–H in-plane bending bands), 839 (aromatic C–H out-of-plane bending bands), 721 (C–S stretching band). ^{1}H NMR (500 MHz, DMSO-d_6), δ: 9.21 (d, J = 2.4 Hz, 1H, pyridine-H), 8.74 (dd, J = 4.8, 1.6 Hz, 1H, pyridine-H), 8.70 (s, 1H, thiazole-H), 8.41 (dd, J = 8, 2.4 Hz, 1H, pyridine-H), 7.60 (dd, J = 8, 4.8 Hz, 1H, pyridine-H), 7.38 (d, J = 8.1 Hz, 2H, Ar-H), 7.14 (d, J = 2.9 Hz, 2H, Ar-H), 4.56 (s, 2H, S-CH_2), 2.27 (s, 3H, CH_3).^{13}C NMR (125 MHz, DMSO-d_6), δ: 21.243, 36.322, 124.937, 125.600, 128.652, 129.574, 129.698, 133.797, 134.622, 137.704, 140.142, 147.696, 152.188, 161.518, 163.985, 166.749. HRMS (*m/z*): $[M+1]^+$ for $C_{18}H_{14}N_4OS_2$ calculated: 367.0682, found: 367.0679.

*2-(2-Chlorobenzylthio)-5-[2-(pyridin-3-yl)thiazol-4-yl]-1,3,4-oxadiazole (**5e**)*

Yield: 65%; mp: 118–123°C; IR $\upsilon_{max}(cm^{-1})$: 3088–2900 (aromatic C–H stretching band), 1638 (C=N stretching band), 1597–1474 (aromatic C=C stretching band), 1086 (C–O–C stretching band), 1173, 1052, 1040, 982 (aromatic C–H in-plane bending bands), 758

(aromatic C–H out-of-plane bending bands), 733 (C–S stretching band). ^{1}H NMR (500 MHz, DMSO-d_6), δ: 9.22 (d, *J* = 2.3 Hz, 1H, pyridine-H), 8.75 (dd, *J* = 4.8, 1.6 Hz, 1H, pyridine-H), 8.72 (s, 1H, thiazole-H), 8.41 (dd, *J* = 8, 2.4 Hz, 1H, pyridine-H), 7.66 (dd, *J* = 7.3, 2.1 Hz, 1H, pyridine-H), 7.63–7.34 (m, 4H, Ar-H), 4.68 (1H, s, S-CH_2). ^{13}C NMR (125 MHz, DMSO-d_6), δ: 34.882, 124.957, 125.753, 128.038, 128.633, 130.178, 130.610, 132.194, 133.874, 134.248, 134.622, 140.084, 147.677, 152.198, 161.768, 163.428, 166.778. HRMS (*m/z*): $[M+1]^+$ for $C_{17}H_{11}N_4OS_2Cl$ calculated: 387.0136, found: 387.0137.

*2-(3-Chlorobenzylthio)-5-[2-(pyridin-3-yl)thiazol-4-yl]-1,3,4-oxadiazole (**5f**)*

Yield:79%; mp: 167–170°C; IR υ_{max}(cm^{-1}): 3065–2900 (aromatic C–H stretching band), 1659 (C=N stretching band), 1589–1474 (aromatic C=C stretching band), 1175, 1046, 983 (aromatic C–H in-plane bending bands), 1090 (C–O–C stretching band), 812, 789 (aromatic C–H out-of-plane bending bands), 723 (C–S stretching band). ^{1}H NMR (500 MHz, DMSO-d_6), δ: 9.16 (d, *J* = 2.2 Hz, 1H, pyridine-H), 8.68 (d, *J* = 4.9 Hz, 1H, pyridine-H), 8.64 (s, 1H, thiazole-H), 8.35 (dt, *J* = 8.0, 2.1 Hz, 1H, pyridine-H), 7.55 (td, *J* = 5.9, 5.5, 4.2 Hz, 2H, pyridine-H, Ar-H), 7.42 (dd, *J* = 5.4, 3.5 Hz, 1H, Ar-H), 7.34–7.29 (m, 2H, Ar-H), 4.54 (s, 2H, S-CH_2). ^{13}C NMR (125 MHz, DMSO-d_6), δ: 35.641, 124.937, 125.638, 128.287, 128.374, 128.633, 129.497, 130.975, 133.499, 134.622, 139.815, 140.113, 147.715, 152.207, 161.768, 163.764, 166.769. HRMS (*m/z*): $[M+1]^+$ for $C_{17}H_{11}N_4OS_2Cl$ calculated: 387.0136, found: 387.0137.

*2-(4-Chlorobenzylthio)-5-[2-(pyridine-3-yl)thiazol-4-yl]-1,3,4-oxadiazole (**5g**)*

Yield: 93%; mp: 155–158°C; IR υ_{max}(cm^{-1}): 3125–2900 (aromatic C–H stretching band), 1603 (C=N stretching band), 1568–1484 (aromatic C=C stretching band), 1075 (C–O–C stretching band), 1162, 1015 (aromatic C–H in-plane bending bands), 808 (aromatic C–H out-of-plane bending bands), 721 (C–S stretching band). ^{1}H NMR (500 MHz, DMSO-d_6), δ: 9.21 (d, *J* = 2.4Hz, 1H, pyridine-H), 8.74 (dd, *J* = 4.8, 1.6 Hz, 1H, pyridine-H), 8.70 (s, 1H, thiazole-H), 8.42–8.39 (m, 1H, pyridine-H), 7.62–7.59 (m, 1H, pyridine-H), 7.53 (d, *J* = 8.5 Hz, 2H, Ar-H), 7.42 (d, *J* = 8.5 Hz, 2H, Ar-H), 4.60 (s, 2H, S-CH_2). ^{13}C NMR (125 MHz, DMSO-d_6), δ: 35.631, 124.937, 125.657, 128.643, 128.911, 129.074, 131.541, 131.733, 132.943, 134.603, 136.302, 140.103, 147.706, 152.207, 161.624, 163.783, 166.759. HRMS (*m/z*): $[M+1]^+$ for $C_{17}H_{11}N_4OS_2Cl$ calculated: 387.0136, found: 387.0145.

*2-(3-Methoxybenzylthio)-5-[2-(pyridin-3-yl)thiazol-4-yl]-1,3,4-oxadiazole (**5h**)*

Yield: 63%; mp: 136–138°C; IR υ_{max}(cm^{-1}): 3055–2900 (aromatic C–H stretching band), 2830 (aliphatic C–H stretching band), 1613 (C=N stretching band), 1586–1474 (aromatic C=C stretching band), 1173, 1055, 1017, 983 (aromatic C–H in-plane bending bands), 1090 (C–O–C stretching band), 777, 698 (aromatic C–H out-of-plane bending bands), 727 (C–S stretching band). ^{1}H NMR (125 MHz, DMSO-d_6), δ: 9.13 (d, *J* = 0.2 Hz, 1H, pyridine C_2-H), 8.64 (d, *J* = 12.1 Hz, 1H, pyridine-H), 8.32 (s, 1H, thiazole-H), 7.53 (tq, *J* = 14.1, 10.3, 3.2 Hz, 1H, pyridine-H), 7.24–6.76 (m, 5H, pyridine-H, Ar-H), 4.49 (s, 2H, S-CH_2), 3.64 (s, 3H, OCH_3). ^{13}C NMR (125 MHz, DMSO-d_6), δ: 36.447, 55.548, 113.813, 115.147, 121.770, 124.928, 125.600, 128.633, 130.255, 134.603, 138.414, 140.142, 147.715, 152.198, 159.781, 161.556, 163.956, 166.759. HRMS (*m/z*): $[M+1]^+$ for $C_{17}H_{11}N_4OS_2Cl$ calculated: 383.0631, found: 383.0626.

4.2 | AChE/BChE Inhibition

The anticholinesterase activity of the compounds was tested on AChE and BChE enzymes according to the slightly modified Ellman method.[68] Human acetylcholinesterase (CAS No: 9000-81-1) and human butyrylcholinesterase (CAS No: 9001-08-5) enzymes were used as enzymes in the assay. Before starting the test process, all solutions were brought to 20–25°C. A total volume of 210 µl was reached in each cell as 140 µl of phosphate buffer, 20 µl of enzyme solution, 20 µl of inhibitor solution, 20 µl of 5,5'-dithio-Bis (2-nitrobenzoic acid) (DTNB) solution, and 10 µl of acetylthiocholine iodide (ATC)/butyrylthiocholine iodide (BTC) solution. The solutions were mixed to form two different test solutions in quantities sufficient for 96 wells. First, the test solution was prepared to include 70 µl of phosphate buffer, 20 µl of enzyme solution, and 20 µl of DTNB solution; the second solution was prepared to contain 70 µl of phosphate buffer and 10 µl of ATC/BTC solution for one well. Initially, the first test solution and inhibitor compound solutions at different concentrations (20 µl) were added to the 96-well plates using the Biotek Precision XS robotic system. Each concentration of inhibitor compounds was applied to the plates in four replicates. Plates were placed in the BioTek-Synergy H1 microplate reader, mixed for 5 min, and then incubated for 15 min at 25°C. At the end of the incubation period, 80 µl of the second test solution in the microplate reader dispenser was added to each well. After the second test solution was added, a rapid mixing process of 30 s was performed. At this stage, the first absorbance reading was taken at 412 nm. The microplates were allowed to mix for an additional 5 min to allow the reaction to continue, after which a second absorbance reading was taken. By taking the absorbance differences between the two readings, the % inhibition rates were calculated according to the following formula:

$$\%\ \text{Inhibition} = (\{[A(K) - A(B)] - [A(I) - A(B)]\}/[A(K) - A(B)]) \times 100, \quad (1)$$

B is the blank (well without adding inhibitor compound and substrate);

K is the control (only the well where no inhibitor compound was added);

A(*B*) is the absorbance reading difference of the blank well;

A(K) is the absorbance reading difference of the control well;

A(*I*) is theabsorbance reading difference of inhibitory substances.

The IC_{50} values of the compounds are calculated from the inhibition curves plotted using the sigmoid dose–response model of the nonlinear regression analysis in Microsoft Office Excel-2013.

4.3 | Molecular docking studies

Molecular docking study was performed using an in silico procedure to define the binding modes of active compounds in the active regions of the enzyme (www.pdb.org, accessed 01 April 2021). X-ray crystal structure of the AChE (PDB ID: 4EY7) was retrieved from the Protein Data Bank server. Schrödinger Maestro[69] interface was used for the molecular docking study and the enzyme crystal was processed using the Protein Preparation Wizard protocol of the Schrödinger Suite 2020. Active compounds were prepared using the LigPrep module[70] to correctly assign the protonation states as well as the atom types. Bond orders were assigned, and hydrogen atoms were added to the structures. The grid generation was formed using the Glide module,[71] and docking runs were performed in standard precision docking mode (SP).

4.4 | MDS studies

MDS has been considered an important computational tool for evaluating the time-dependent stability of the ligand–receptor complex. In this study, MDS for 50 ns was carried out to ensure the stability of the identified hits from the docking results. We performed Desmond application[66] using the standard force field (OPLS3e) of Schrodinger Suite with a transferable intermolecular potential with 3 points (TIP3P) water model followed by energy minimization of the complex. The neutralization of the system was achieved using Na^+ and Cl^- ions and 150 mM NaCl was added to the dynamic condition. The MDS was performed following the completion of the system setup. The radius of gyration (Rg), root mean square fluctuation (RMSF), and root mean square deviation (RMSD) values were calculated by the Desmond application.

4.5 | ADME parameters

In silico ADME, pharmacokinetics, and drug-likeness properties of the final compounds were predicted using the SwissADME software program. NBA, NBD, TPSA, Log P were calculated, and GI level and level of crossing the BBB of the compounds were estimated.[72]

ACKNOWLEDGMENTS

This study was supported by the Scientific Research Projects Fund of Eskişehir Osmangazi University by the project number: 202019A106. The authors gratefully acknowledge the financial support from Eskişehir Osmangazi University.

CONFLICTS OF INTEREST

The authors declare no conflicts of interest.

ORCID

Asaf E. Evren http://orcid.org/0000-0002-8651-826X
Leyla Yurttaş http://orcid.org/0000-0002-0957-6044
Naime F. Tay http://orcid.org/0000-0002-5765-8212

REFERENCES

[1] D. De Boer, N. Nguyen, J. Mao, J. Moore, E. J. Sorin, *Biomolecules* **2021**, *11*, 580.
[2] S. Askın, H. Tahtacı, C. Türkeş, Y. Demir, A. Ece, G. Akalın Çiftçi, Ş. Beydemir, *Bioorg. Chem.* **2021**, *113*, 105009.
[3] T. Zorbaz, A. Braïki, N. Maraković, J. Renou, E. de la Mora, N. Maček Hrvat, M. Katalinić, I. Silman, J. L. Sussman, G. Mercey, *Chem. - Eur. J.* **2018**, *24*, 9675.
[4] Z. Kovarik, J. Kalisiak, N. M. Hrvat, M. Katalinić, T. Zorbaz, S. Zunec, C. Green, Z. Radić, V. V. Fokin, K. B. Sharpless, *Chem. - Eur. J.* **2019**, *25*, 4100.
[5] M. B. Colovic, D. Z. Krstic, T. D. Lazarevic-Pasti, A. M. Bondzic, V. M. Vasic, *Curr. Neuropharmacol.* **2013**, *11*, 315.
[6] J. A. Miles, J. H. Ng, B. Y. Sreenivas, C. Courageux, A. Igert, J. Dias, R. P. McGeary, X. Brazzolotto, B. P. Ross, *Chem. Biol. Drug Des.* **2021**, *97*, 1048.
[7] M. Mehta, A. Adem, M. Sabbagh, *Int. J. Alzheimer's Dis.* **2012**, *2012*, 728983.
[8] M. Pohanka, *Int. J. Mol. Sci.* **2014**, *15*, 9809.
[9] S. Ruangritchankul, P. Chantharit, S. Srisuma, L. C. Gray, *Ther. Clin. Risk. Manag.* **2021**, *17*, 927.
[10] A. L. Guillozet, J. F. Smiley, D. C. Mash, M. M. Mesulam, *Ann. Neurol.* **1997**, *42*(6), 909.
[11] E. Giacobini, *Drugs Aging* **2001**, *18*(12), 891.
[12] M. Weinstock, *CNS Drugs* **1999**, *12*(4), 307.
[13] S. Young, E. Chung, M. A. Chen, *Ann. Geriatr. Med. Res.* **2021**, *25*(3), 170.
[14] M. Mehrponya, S. Ataei, A. Nili-Ahmadabadi, *J. Appl. Pharm* **2017**, *7*(1), 223.
[15] M. R. Farlow, S. Salloway, P. N. Tariot, J. Yardley, M. L. Moline, Q. Wang, E. Brand-Schieber, H. Zou, T. Hsu, A. Satlin, *Clin. Ther.* **2010**, *32*, 1234.
[16] B. David, P. Schneider, P. Schafer, J. Pietruszka, H. Gohlke, *J. Enzyme Inhib. Med. Chem.* **2021**, *36*(1), 491.
[17] J. P. Rowland, J. Rigby, A. C. Harper, R. Rowland, *Adv. Psychiatr. Treat.* **2007**, *13*, 178.
[18] J. G. Evans, G. Wilcock, F. Birks, *Int. J. Neuropsychopharmacol.* **2004**, *7*, 351.
[19] A. G. Zaki, R. El-Sayed, M. Abd Elkodous, G. S. El-Sayyad, *Appl. Microbiol. Biotechnol.* **2020**, *104*, 4717.
[20] Ş. Demirayak, Z. Şahin, M. Ertaş et al., *J. Heterocyclic Chem.* **2019**, *56*(12), 1.
[21] Z. Sahin, S. N. Biltekin, E. F. Bülbül, L. Yurttas, B. Berk, Ş. Demirayak, *Phosphorus Sulfur Silicon Relat. Elem.* **2021**, *196*, 283.
[22] D. Kumar, S. Sundaree, E. O. Johnson, K. Shah, *Bioorg. Med. Chem. Lett.* **2009**, *19*, 4492.
[23] J. A. Ahsan, A. Choupra, R. K. Sharma, S. S. Jadav, P. Padmaja, M. Z. Hassan, A. B. S. Al-Tamimi, M. H. Geesi, M. A. Bakht, *Anticancer Agents. Med. Chem.* **2018**, *18*, 121.
[24] E. Palaska, G. Sahin, P. Kelicen, N. T. Durlu, G. Altinok, *Farmaco* **2002**, *57*(2), 101.
[25] F. A. Omar, N. M. Mahfouz, M. A. Rahman, *Eur. J. Med. Chem.* **1996**, *31*(10), 819.
[26] M. Akhter, A. Husain, B. Azad, M. Ajmal, *Eur. J. Med. Chem.* **2009**, *44*(6), 2372.

[27] B. Chandrakantha, P. Shetty, V. Nambiyar, N. Isloor, *Eur. J. Med. Chem.* **2010**, *45*, 1206.
[28] M. S. Karthikeyan, D. J. Parsad, M. Mahalinga, B. S. Holla, N. S. Kumari, *Eur. J. Med. Chem.* **2008**, *43*, 25.
[29] S. A. Shahzad, M. Yar, M. Bajda, B. Jadoon, Z. A. Khan, S. A. R. Naqvi, A. J. Shaikh, K. Hayat, A. Mahmmoda, N. Mahmood, S. Filipek, *Bioorg. Med. Chem.* **2014**, *22*, 1008.
[30] S. Dash, B. A. Kumar, J. Singh, B. C. Maiti, T. K. Maity, *Med. Chem. Res.* **2011**, *20*, 1206.
[31] S. Viveka Dinesha, P. Shama, G. K. Nagaraja, N. Deepa, M. Y. Sreenivasa, *Res. Chem. Intermed.* **2016**, *42*, 2597.
[32] S. Viveka Dinesha, S. Chandra, G. K. Nagaraja, *Monatsh. Chem.* **2015**, *146*, 207.
[33] J. Iqbal, A. Rehman, M. A. Abbasi, S. Z. Siddiqui, S. Rasool, M. Ashraf, A. Iqbal, S. Hamid, T. A. Chohan, H. Khalid, S. J. Laulloo, S. A. A. Shah, *iD Braz. J. Pharm. Sci.* **2020**, 56.
[34] R. Mirzazadeh, M. S. Asgari, E. Barzegari, K. Pedrood, M. Mohammadi-Khanaposhtani, M. Sherafati, B. Larijani, H. Rastegar, H. Rahmani, M. Mahdavi, P. Taslimi, E. M. Üç, İ. Gulçin, *Arch. Pharm.* **2021**, *354*, 2000471.
[35] Q. Z. Zheng, X. M. Zhang, Y. Xu, K. Cheng, Q. C. Jiao, H. L. Zhu, *Bioorg. Med. Chem.* **2010**, *18*, 7836.
[36] M. A. Abbasi, M. S. Ramzan, A. Ur-Rehman, S. Z. Sıddıqui, M. Hassan, H. Raza, S. A. A. Shah, B. Mırza, S. Y. SEO, *J. Serb. Chem. Soc.* **2019**, *84*(7), 649.
[37] F. Fumagalli, S. M. G. de Melo, C. M. Ribeiro, M. C. Solcia, F. R. Pavan, F. S. Emery, *Bioorg. Med. Chem. Lett.* **2019**, *29*, 974.
[38] S. Yasodakrishna, V. Hanmanth Reddy, B. Rajashaker, N. Lingaiah, V. Sathish Babu, K. Srigiridhar, N. Jagadeesh Babu, *Bioorg. Med. Chem. Lett.* **2016**, *26*, 858.
[39] G. S. Kumar, Y. Poornachandra, G. S. Kumar, K. R. Reddy, M. Jaheer, S. Kamal, C. G. Kumar, B. Narsaiah, *Bioorg. Med. Chem. Lett.* **2018**, *28*, 2328.
[40] M. V. K. Reddy, K. Y. Rao, G. Anusha, G. M. Kumar, A. G. Damu, K. G. Reddy, N. P. Shetti, T. M. Aminabhavi, P. V. G. Reddy, *Environ. Res.* **2021**, *199*, 111320.
[41] A. Tripathi, P. K. Choubey, P. Sharma, A. Seth, P. N. Tripathi, M. K. Tripathi, S. K. Prajapati, S. Krishnamurthy, S. K. Shrivastava, *Eur. J. Med. Chem.* **2019**, *183*, 111707.
[42] H. Zhang, C. Wu, X. Chen, Z. Zhang, X. Jiang, H. L. Qin, W. Tang, *ChemMedChem* **2021**, *16*, 3189.
[43] N. Bulut, U. M. Kocyigit, I. H. Gecibesler, T. Dastan, H. Karci, P. Taslimi, S. D. Dastan, I. Gulcin, A. Cetin, *J. Biochem. Mol. Toxicol.* **2018**, *32*, 22006.
[44] B. Barut, H. Baş, Z. Bıyıklıoğlu, *Turk. J. Chem.* **2021**, *45*, 1567.
[45] S. Zarei, M. Shafiei, M. Firouzi, L. Firoozpour, K. Divsalar, A. Asadipour, T. Akbarzadeh, A. Foroumadi, *Heliyon* **2021**, *7*, e06683.
[46] Y. Ling, Z. Y. Hao, D. Liang, C. L. Zhang, Y. F. Liu, Y. Wang, *Drug. Des. Devel. Ther.* **2021**, *15*, 4289.
[47] R. Sekioka, S. Honda, H. Akashiba, J. Yarimizu, Y. Mitani, S. Yamasaki, *Bioorg. Med. Chem.* **2020**, *28*, 115455.
[48] R. Ghobadian, M. Mahdavi, H. Nadri, A. Moradi, N. Edraki, T. Akbarzadeh, M. Amini, *Eur. J. Med. Chem.* **2018**, *155*, 49.
[49] T. Umar, S. Shalini, M. K. Raza, S. Gusain, J. Kumar, P. Seth, N. Hoda, *Eur. J. Med. Chem.* **2019**, *175*, 2.
[50] M. H. Hannoun, M. Hagras, A. Kotb, A. A. M. M. El-Attar, H. S. Abulkhair, *Bioorg. Chem.* **2020**, *94*, 103364.
[51] N. C. Desai, N. Bhatt, H. Somani, A. Trivedi, *Eur. J. Med. Chem.* **2013**, *67*, 54.
[52] N. C. Desai, N. Bhatt, H. Somani, *Med. Chem. Res.* **2015**, *24*, 258.
[53] M. Zia, T. Akhtar, S. Hameed, N. A. Al-Masoudi, *Z. Naturforsch.* **2012**, *67b*, 747.
[54] F. Rahim, M. T. Javed, H. Ullah, A. Wadood, M. Taha, M. Ashraf, Q. ul-Ain, M. A. Khan, F. Khan, S. Mirza, K. M. Khan, *Bioorg. Chem.* **2015**, *62*, 106.
[55] G. F. Makhaeva, N. P. Boltneva, S. V. Lushchekina, O. G. Serebryakova, T. S. Stupina, A. A. Terentiev, I. V. Serkov, A. N. Proshin, S. O. Bachurin, R. J. Richardson, *Bioorg. Med. Chem.* **2016**, *24*, 1050.
[56] A. Y. Hemaida, G. S. Hassan, A. R. Maarouf, J. Joubert, A. A. El-Emam, *ACS Omega* **2021**, *6*, 19202.
[57] Z. Sahin, M. Ertas, C. Bender, E. F. Bülbül, B. Berk, S. N. Biltekin, L. Yurttas, Ş. Demirayak, *Drug Dev. Res.* **2018**, *79*, 406.
[58] B. N. Saglık, D. Osmaniye, U. Acar Çevik, S. Levent, B. Kaya Çavusoglu, Y. Özkay, Z. A. Kaplancıklı, *Molecules* **2020**, *25*, 4312.
[59] R. K. P. Tripathi, M. V. Sasi, S. K. Gupta, S. Krishnamurthy, S. R. Ayyannan, *J. Enzyme Inhib. Med. Chem.* **2018**, *33*, 37.
[60] X. Z. Zhang, Y. Xu, M. M. Jian, K. Yang, Z. Y. Ma, *Med. Chem. Res.* **2019**, *28*, 1683.
[61] Y. Xu, M. M. Jian, C. Han, K. Yang, L. Bai, F. Cao, Z. Y. Ma, *Bioorg. Med. Chem. Lett.* **2020**, *30*, 126985.
[62] A. Luqman, V. L. Blair, R. Brammananth, P. K. Crellin, R. L. Coppel, P. C. Andrews, *Eur. J. Inorg. Chem.* **2015**, *29*, 4935.
[63] S. T. Dhumal, A. R. Deshmukh, M. R. Bhosle, V. M. Khedkar, L. U. Nawale, D. Sarkar, R. A. Mane, *Bioorg. Med. Chem. Lett.* **2016**, *26*, 3646.
[64] F. Tay, B. Berk, M. Duran, İ. Kayagil, L. Yurttas, S. N. Biltekin Kaleli, M. Yamaç, A. B. Karaduman, Ş. Demirayak, *Z. Naturforsch. C* **2022**. https://doi.org/10.1515/znc-2022-0002
[65] Ş. Durmaz MSc Thesis, University of Eskişehir Osmangazi University, (Eskişehir, Turkey) **2021**.
[66] Desmond Molecular Dynamics System. D. E. Shaw Research. New York, NY 2021. *Maestro-Desmond Interoperability Tools*, Schrödinger, New York, NY, **2020**. https://www.schrodinger.com/products/desmond
[67] C. A. Lipinski, F. Lombardo, B. W. Dominy, P. J. Feeney, *Adv. Drug Deliv. Rev.* **2001**, *46*, 3.
[68] G. L. Ellman, K. D. Courtney, V. Andres, R. M. Feather-Stone, *Biochem. Pharmacol.* **1961**, *7*(2), 88.
[69] Maestro. Schrödinger, Schrödinger Release 2020-3. Schrödinger, LLC, New York, NY. **2020**. https://www.schrodinger.com.tr/products/maestro
[70] LigPrep. Schrödinger, Schrödinger Release 2020-3. Schrödinger, LLC, New York, NY. **2020**. https://www.schrodinger.com.tr/products/ligprep
[71] Glide. Schrödinger, Schrödinger Release 2020-3. Schrödinger, LLC, New York, NY. **2020**. https://www.schrodinger.com.tr/products/glide
[72] SwissADME: a free web tool to evaluate pharmacokinetics, drug-likeness and medicinal chemistry friendliness of small molecules. Sci. Rep. **2017**, *7*, 42717. http://www.swissadme.ch/Last (accessed November 2021).

SUPPORTING INFORMATION

Additional supporting information can be found online in the Supporting Information section at the end of this article.

How to cite this article: Ş. Durmaz, A. E. Evren, B. N. Sağlık, L. Yurttaş, N. F. Tay, *Arch. Pharm.* **2022**;355:e2200294. https://doi.org/10.1002/ardp.202200294